  Bull. Chem. Soc. Jpn., 64, 3620—3626 (1991)

ENDOR and TRIPLE Studies of Diphenyl Nitroxide (DPNO)

Jun YAMAUCHI,* Hideo FUJITA, and Yasuo DEGUCHI
College of Liberal Arts and Sciences, Kyoto University, Kyoto 606
(Received July 8, 1991)

ENDOR and triple resonance (GTR) of diphenyl nitroxide (DPNO) were observed in solution; it was demonstrated that DPNO is an interesting model radical forming a three-spin system (electron and ^{1}H- and ^{14}N-nuclear spins). The detected ^{14}N-ENDOR belongs to one of the smallest hyperfine cases (A_N=0.9653 mT). Its optimum temperature was 210 K, higher than that of the ^{1}H, which is due to the large anisotropic hyperfine interaction of ^{14}N. In the ^{1}H-ENDOR spectra the effect of cross relaxation was observed, as in the case of the ^{14}N-ENDOR lines; their temperature variations of intensity showed two maximum regions, one due to the optimum energy relaxation in the ^{14}N-spin system and the other due to the energy relaxation inherent in the ^{1}H-spin system. In the triple studies new phenomena were pointed out: An enhancement saturation effect due to the large hyperfine interaction and an intensified enhancement or de-enhancement effect due to the cross relaxation.

In investigations of electron spin resonance (ESR) spectroscopy and its applications to chemistry, diphenyl nitroxide (DPNO) has been used as a model radical for a few decades. The reason may be that DPNO is not only facile in handling, but also it can afford an interesting spin system consisting of an electron spin and two nuclear spins, ^{1}H and ^{14}N. ESR experiments of DPNO were first performed using single crystals, and some variations of exchange narrowed lines were measured by changing the magnitude of magnetic dilution in crystals.[1] Then, well-resolved ^{1}H-hyperfine spectra were observed in order to calculate the linewidth of each hyperfine line.[2] It was also reported that dissolved oxygen in solvents plays a remarkable negative role in diminishing the ^{1}H-hyperfine lines.[3] Some of the present authors et al. have investigated the repulsion scheme between the two ortho-protons of DPNO and the effect of methyl substitution on the ortho-positions of DPNO.[4]

In an electron-nuclear double-resonance (ENDOR) study, on the other hand, DPNO and its methyl derivatives have been investigated in detail from the point of view of steric hindrance.[5] An extension of ENDOR to a general triple resonance (GTR) for DPNO has been attempted in order to assure a negative spin density on the carbon atoms at the meta-positions of DPNO, demonstrating the typical GTR behavior in the spectral intensity change.[6] In these double- and triple-resonance investigations, no ^{14}N signals or a responce have been observed, in spite of the largest hyperfine coupling constant (A_N=0.965 mT) in this system.

Some nitroxide radicals have been investigated extensively with regard to ^{14}N-ENDOR detections.[7] The first observation was accomplished by Leniart et al. for some alicyclic nitroxide radicals.[8] We recently reported on ^{1}H- and ^{14}N-ENDOR studies of *t*-butylphenyl nitroxide (BPNO).[9] In these investigations, the characteristic features in ^{14}N-ENDOR were pointed out, such as cross relaxations in the ^{14}N-ENDOR and the influence of the ^{14}N-spin quantum number on the ^{1}H-ENDOR patterns. In this report we focus attention on ^{14}N-ENDOR observations of DPNO, the temperature dependences of the ^{14}N- and ^{1}H-ENDOR lines, and the ^{1}H-GTR characteristics of the radio-frequency power variations; we discuss especially how the ^{1}H-ENDOR and GTR are influenced by the ^{14}N-spin system. Success involving the ^{14}N-ENDOR detection would again shed light on DPNO as an interesting model sample in both double- and triple-resonance spectroscopies, in which three interacting spins (the electron spin and ^{1}H- and ^{14}N-nuclear spins) play an important role in the energy relaxations.

Experimental

Samples were synthesized as described in a previous paper.[4] For the ENDOR measurements, freshly prepared DPNO gave satisfactory results. Therefore, we used the following procedure. The synthesized DPNO was diluted magnetically in a diamagnetic matrix of benzophenone; this solid solution was kept in a refrigerator. Just before sampling for the measurements, pure DPNO was separated by chromatography.

A broad-band ENDOR spectrometer equipped with a TM_{110} mode cavity was used as described previously.[5] Two signal generators, i.e. HP8601A (Hewlett-Packard) and VP-8179B10 (National), were used for scanning the radio-frequency with FM modulation (6.5 kHz) and pumping the radio-frequency without FM modulation, respectively.[6] The experimental conditions of the multiple resonances are as follows: for the ^{14}N-ENDOR observed at 220 K, a microwave power of 20 mW and a radio-frequency power of 100 W were used; for the ^{1}H-GTR measured at 180 K, a microwave power of 20 mW and a scanning radio-frequency power of 80 W were used. The pumping radio-frequency power was changed between 0—100 W. Ethylbenzene or toluene was used as a solvent and the temperature was controlled by a JEOL ES-DVT2 between 160—230 K.

Results

In the ENDOR measurements, although two pairs of ^{1}H signals centered at the free-proton frequency (14.196 MHz) were usually detected within the observed temperature region, the optimum temperature was found to be

180 K (see Fig. 2 in the literature[6]).

The inner pair at 13.044 and 15.348 MHz was assigned to the meta-protons with a hyperfine coupling constant, A_{Hm}=0.082 mT. The outer one at 11.512 and 16.881 MHz is attributable to the ortho- and para-protons of A_{Ho}=A_{Hp}=0.191 mT. Hereafter, the ENDOR absorption lines are designated as **a'**, **b'**, **b**, and **a** from the low-frequency side, respectively. The temperature dependence of the signal intensities of each line between 170—230 K is plotted in Fig. 1.

For the ^{14}N-ENDOR observation the experimental conditions were carefully chosen with regard to both the microwave and radio-frequency powers, temperature, and sample concentration. The solvents were not varied except for toluene and ethylbenzene. The temperature was found to be optimum at about 210 K, rather higher than in the detection of ^{1}H-ENDOR. The lower sample concentration seemed to be better for accomplishing easy saturation and low-noise detection of the 80 Hz ESR. Figure 2 shows the ^{1}H- and ^{14}N-ENDOR spectra observed at 220 K in a toluene solution. The newly appearing one pair of signals between the ^{1}H-ENDOR lines (**a'**, **b'**, and **b'**, **b**) was assigned to the ^{14}N-ENDOR lines. Spectra (a), (b), and (c) in Fig. 2 indicate ENDOR pattern variations due to the nitrogen nuclear quantum

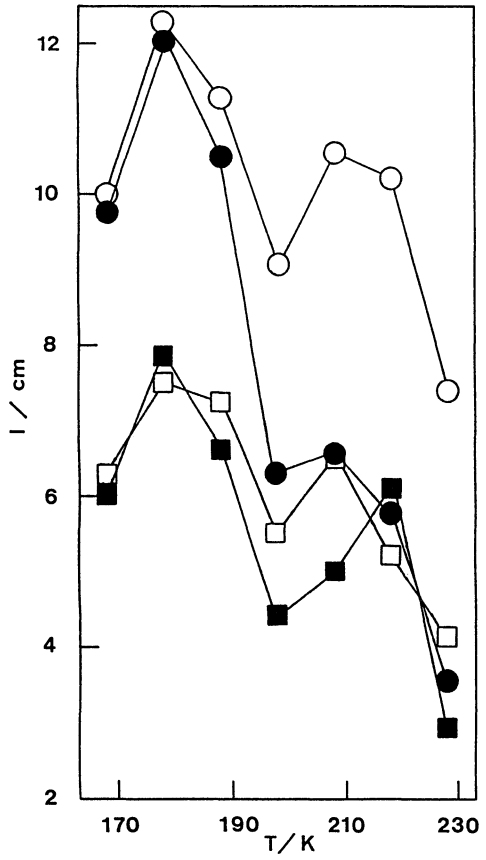

Fig. 1. Intensity variations of the ^{1}H-ENDOR lines taken as a peak-to-peak height. ○ and ● indicate the outer paired lines (**a** and **a'**), and □ and ■ the inner ones (**b** and **b'**).

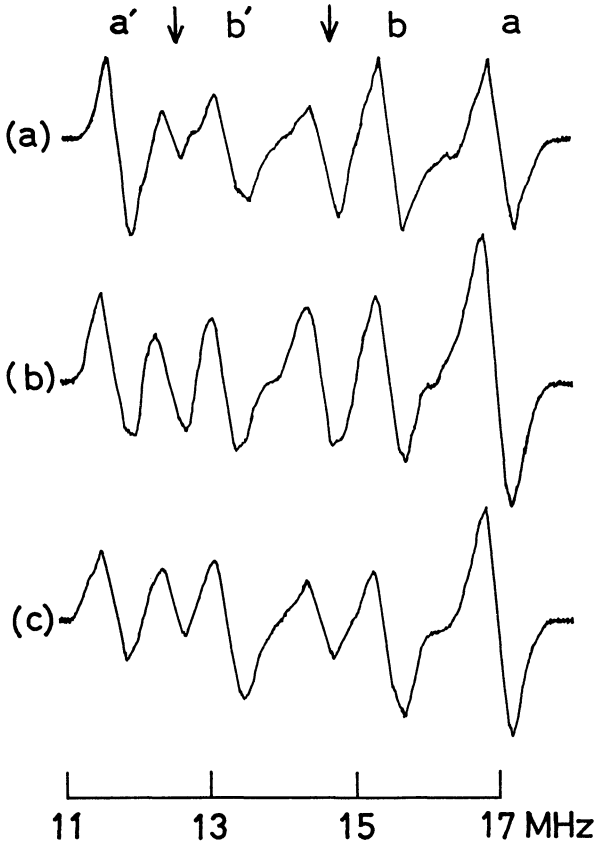

Fig. 2 ^{14}N- and ^{1}H-ENDOR spectra of DPNO observed in toluene at 220 K. The arrows indicate the ^{14}N-ENDOR lines. In these ENDOR observations ESR was monitored at the low-field ESR m_I=1 (**a**), the central ESR m_I=0 (**b**), and the high-field ESR m_I=−1 (**c**).

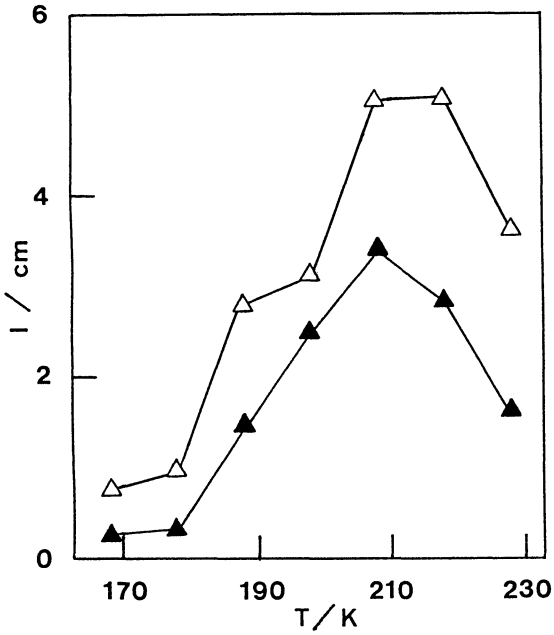

Fig. 3. Intensity variations of the ^{14}N-ENDOR lines taken as a peak-to-peak height. △ and ▲ indicate the high- and low-frequency lines, respectively.

numbers (m_I=1, 0, and −1) where the ESR was monitored.[10] The spectral intensity change of Fig. 2-(b) vs. temperature was shown in Fig. 3.

In the GTR measurements each of the ^{1}H-ENDOR lines was pumped using the second radio-frequency power; then, the other ^{1}H-ENDOR lines were influenced regarding their absorption intensity (see Fig. 2 in the literature[6]). The intensity variations measured at 180 K are plotted against the pumping radio-frequency power in Figs. 4 and 5. The GTR behaviors were the most

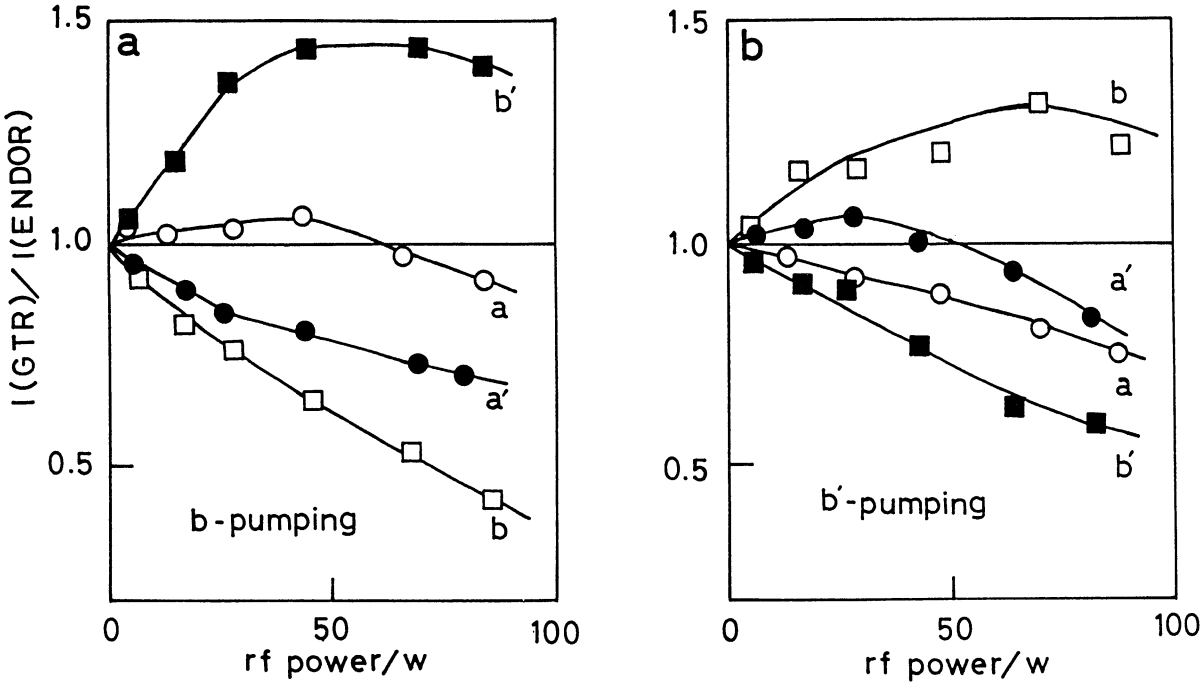

Fig. 4. Enhancement and de-enhancement of the GTR spectra with the inner paired ^{1}H-ENDOR lines (**b** and **b'**) pumped by the radio-frequency powers in the abscissa scale. ESR monitoring was set on the m_I=0 component. (See text concerning the ordinate scale.)

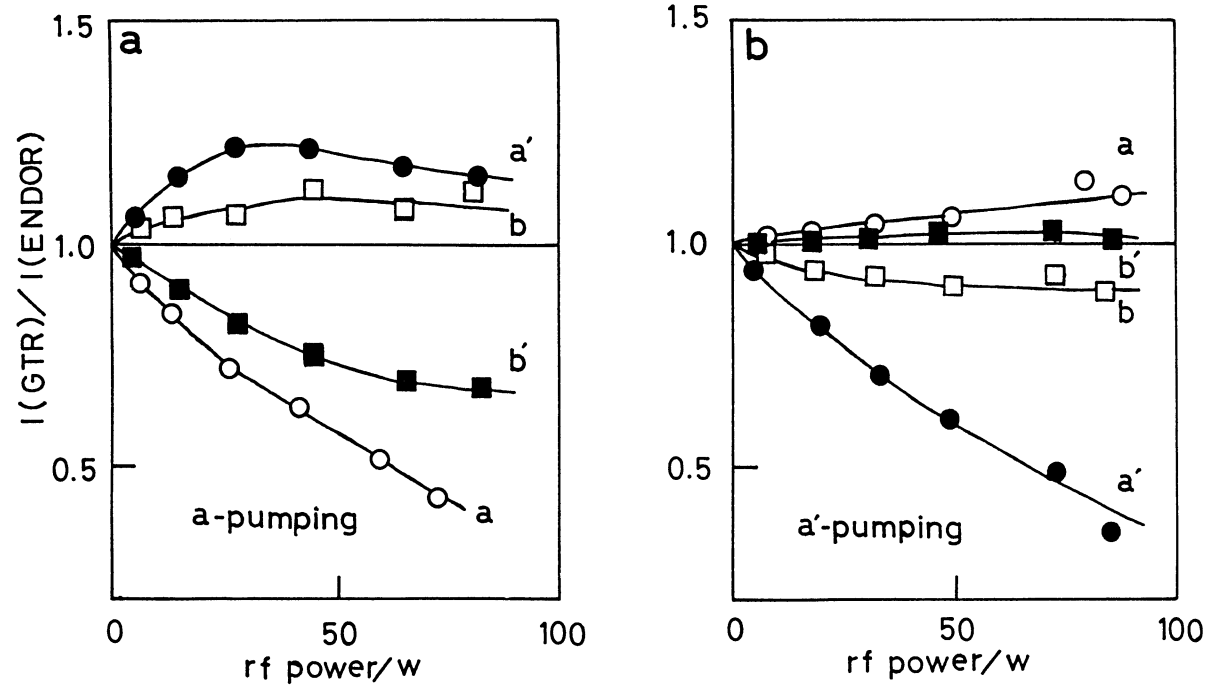

Fig. 5. Enhancement and de-enhancement of the GTR spectra with the outer paired ^{1}H-ENDOR lines (**a** and **a'**) pumped by the radio-frequency powers in the abscissa scale. ESR monitoring was set on the m_I=0 component. (See text concerning the ordinate scale.)

remarkable at the optimum temperature of the ^{1}H-ENDOR (180 K). The spectral enhancement or de-enhancement of the GTR spectra was not emphasized at the optimum temperature of the ^{14}N-ENDOR (210 K), probably due to complicated energy relaxations in the ^{14}N- and ^{1}H-nuclear spin systems, as discussed later. The data in Figs. 4 and 5 were obtained by monitoring the ESR of the m_I=0 component. If we changed the ESR observation to those of m_I=1 or −1, the intensity variations were slightly influenced, as is also discussed later.

Discussion

^{14}N-ENDOR Spectra. The newly appearing lines among the ^{1}H-ENDOR lines can be assigned to the ^{14}N-ENDOR absorptions, because of a separation of the two lines corresponding to $2\nu_N$, where ν_N is the nitrogen nuclear-magnetic-resonance frequency. Therefore, the average frequency of the paired lines is equal to the ^{14}N hyperfine coupling constant, A_N=0.9653 mT, which is in good agreement with the value A_N=0.965 mT determined from the ESR at 188 K in toluene.

The ^{14}N hyperfine coupling constant, A_N=0.9653 mT, is among the smaller values found in ENDOR observations of nitroxide radicals. It is usually true that the lower is the hyperfine coupling constant, the more difficult it is to be detected. Our observation is presently a lower-limit case of the nitroxide radicals. There have been several ^{14}N-ENDOR observations reported for other types of radicals with a smaller ^{14}N hyperfine interaction.[11,12] The difference may be associated with energy relaxation due to an anisotropic hyperfine interaction Tr $\{A'^2\}$, which is described below.

The higher optimum temperature of the ^{14}N-ENDOR (Fig. 3) is attributable to the different anisotropic hyperfine interactions of the ^{14}N and ^{1}H nuclei. In general, the calculated ENDOR signal can be expressed by τ_R and Tr$\{A'^2\}$, based on certain assumptions, where τ_R is the rotational correlation time of the molecule and Tr$\{A'^2\}$ is the trace of the squared anisotropic part of the electron-nuclear dipolar interaction.[11] The anisotropic ^{14}N hyperfine interaction, Tr$\{A'^2\}$, for nitroxide radicals, such as DPNO, is Tr$\{A'^2\}$=2200 MHz^2; whereas that of the ^{1}H, which is attached to the benzene ring, is about 30 MHz^2.[1,13] This difference explains the higher optimum temperature of the ^{14}N-ENDOR.

The ^{14}N-ENDOR lines indicated by the arrows in Fig. 2 show the spectral intensity change depending on ESR monitoring. This phenomenon was first pointed out by Leniart et al.,[8] and could be explained in terms of cross relaxation W_{X1} and W_{X2} depicted in Fig. 6. For instance, when one is sitting on the higher or lower field component of the ESR (m_I=−1 or +1) in the ENDOR observations, the energy relaxation is governed by the W_{X1}, W_{X2}, ω_{n1}, and ω_{n2} transitions associated with the central components of the energy levels. Accordingly, the high- and low-frequency ENDOR absorptions

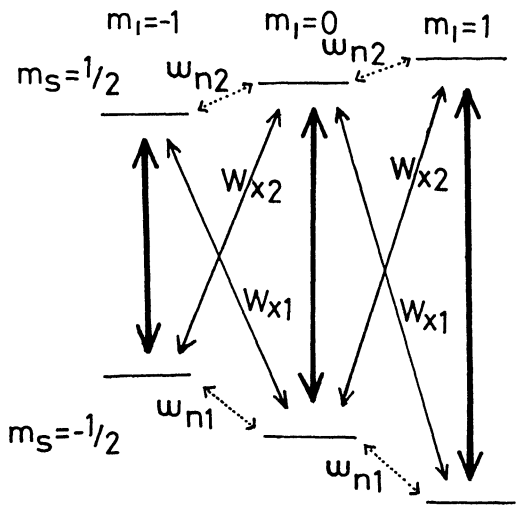

Fig. 6. Energy diagram of the unpaired electron (m_S=1/2, −1/2) and the ^{14}N nucleus (m_I=1, 0, −1). The cross relaxations W_{X1} and W_{X2} relate the transitions $\Delta(m_S+m_I)$=0 and $\Delta(m_S+m_I)$=±2, respectively. The high- and low-frequency ENDOR absorptions correspond to ω_{n1} and ω_{n2}, respectively. This diagram is depicted for the case of a positive hyperfine interaction A_N>0.

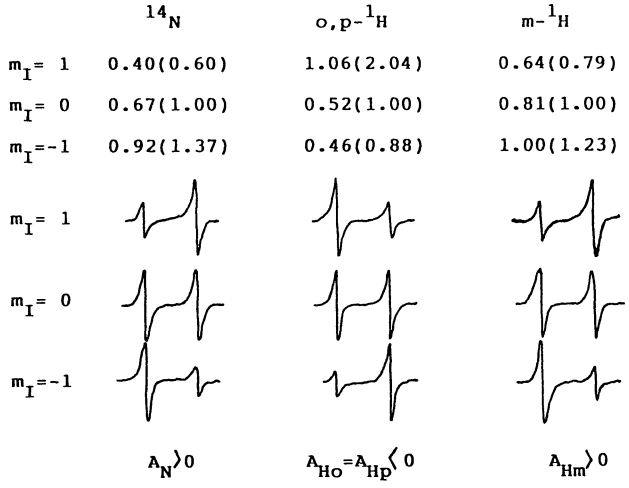

Fig. 7. Intensity ratio and its variations of each paired line for the ESR monitoring on m_I=1, 0, and −1. The schematic paired lines are depicted on the basis of the normalized intensity ratios (values in the parentheses). The meta-protons behave like the ^{14}N, whereas the ortho- and para-protons behave in an opposite way, leading to A_{Hm}>0 and A_{Ho}=A_{Hp}<0.

(ω_{n1} and ω_{n2}, respectively) show different spectral intensities due to the different W_{X1} and W_{X2} values. On the other hand, the central energy levels, which belong to m_I=0 component, can dissipate their energy to both sides. As a result, the high- and low-frequency ENDOR lines are averaged in intensity. The ^{14}N-ENDOR intensity changes with the m_I values are tabulated in Fig. 7. The values indicate the intensity ratio between the low- and high-frequency components; those

in the parentheses were normalized ones by the intensity ratio of $m_I=0$. The intensity patterns shown schematically in Fig. 7 indicate a positive hyperfine coupling constant of the ^{14}N nucleus, as is supposed in Fig. 6. Interestingly, these ^{14}N-cross relaxations also influence the ^1H-energy relaxation, as is summarized in Fig. 7. This is discussed next.

^1H-ENDOR Spectra. The ^1H-ENDOR lines are rather broad at 220 K, but the intensity changes with the m_I values are clear (Fig. 7). This effect was first pointed out by Janzen et al.[14] and independently by us,[15] and is referred to CRISP (cross relaxation intensity sequence pattern). The spectral intensity changes are opposite for the ortho- or para-protons and the meta-protons. This means the opposite signs of the hyperfine coupling constants (that is, $A_{Ho}=A_{Hp}<0$ and $A_{Hm}>0$) because the energy levels in Fig. 6 are reversed, depending on the signs of the hyperfine coupling constants. We can therefore conclude a negative spin density at the meta-positions of the phenyl rings, which agrees with the conclusion derived from the GTR results. The strong and weak intensity sequence patterns become important regarding the GTR behaviors on the spectral enhancement or de-enhancement.

The influence of the ^{14}N-energy relaxation on the ^1H-nuclear system was also ascertained by the temperature dependences of the ^1H-ENDOR lines. Figure 1 shows the intensities of the ^1H lines of the ENDOR spectra ($m_I=0$) at various temperatures. There are two characteristic features. One is the fact that there are two maximum regions; the other is the good coincidence of the intensity of each paired line at the lowest temperature region. Comparing these results with those of the ^{14}N-ENDOR lines (Fig. 3), one can easily conclude that the first maximum region around 210 K is somewhat related to the optimum temperature of the ^{14}N-ENDOR lines. This means that the effective energy relaxation in the ^{14}N-spin system at this temperature might cause a sufficient energy relaxation in the ^1H-spin system. As a matter of fact, the optimum conditions inherent in the ^1H-spin system are fulfilled at the lower temperatures, exhibiting a second maximum at 180 K. This finding implies the existence of a coupling between the ^{14}N and ^1H nuclei through the electron spin or through a direct interaction.[16] The meaningful effect of the nuclear–nuclear coupling was first pointed out concerning this ENDOR intensity. In addition to the CRISP effect, this is another interesting point regarding a three-spin system comprising one electron and two nuclear spins (^1H and ^{14}N). In the case of a three-spin system with similar nuclei (for instance, two non-equivalent protons), the energy relaxations becomes optimum at almost the same temperature regions, resulting in one maximum. The essential point in our spin system is two different nuclei (^{14}N and ^1H) which have optimum energy relaxation at different temperatures.

The second feature of Fig. 1 can also be explained by the above-mentioned interaction. At lower temperatures the ^{14}N-energy relaxation becomes ineffective and the original characteristics of the pure ^1H-spin system appear. Therefore, approaching the ^1H-optimum temperature region, the intensity of each paired line becomes the same as that shown in Fig. 1. As for this new finding, one comment is noteworthy concerning the previous experiment of BPNO.[9] The temperature dependence of the ENDOR intensities of the ^1H and ^{14}N absorptions were not analyzed in this way. The correct interpretation should be as follows. The first optimum region of the ^1H lines appeared at $-60\,^\circ C$, roughly corresponding to the maximum of the ^{14}N intensity. In BPNO, however, no second maximum, which is originally characteristic of the ^1H nuclei, was found over the observed temperature range (above $-90\,^\circ C$).

Triple Resonance Spectra. Figures 4 and 5 show the intensity variations of the GTR spectra by the pumping radio-frequency power. The spectral enhancement was defined by $I(GTR)/I(ENDOR)$, where $I(GTR)$ and $I(ENDOR)$ are the spectral intensity taken as absorption height with and without the pumping radio-frequency power, respectively. According to the results given in Figs. 4 and 5, one can conclude the opposite signs for the hyperfine coupling constants of the meta- and the ortho- or para-protons, since the inner paired lines (**b′** and **b**) as well as the outer ones (**a′** and **a**) change oppositely in intensity.[17] For instance, in Fig. 4, upon pumping one of the inner pair (**b′**), an enhancement took place on the high-frequency partner (**b**); on the outer paired lines, however, the high-frequency line **a** decreased and the low-frequency one **a′** was enhanced, though its enhancement was quite small. This situation is fully inversed to the case of pumping one of the inner lines, **b**. These observations are also the same for the cases of **a** and **a′** pumping (Fig. 5).

We next consider the enhancement or de-enhancement values. The radio-frequency pumping effect is always clear for the de-enhancement case, whereas the behavior in the enhancement situation is sometimes smeared out and the intensity enhancement is cancelled in the high radio-frequency power region, which may be referred to as enhancement "saturation". Since this tendency seems to be remarkable concerning the outer pair, one of the reasons for this enhancement saturation may be the large hyperfine coupling constant of the ortho- or para-protons, as compared with that of the meta-protons. This effect can be called a radio-frequency enhancement effect at the nucleus through a hyperfine interaction. An intensity enhancement saturation is therefore likely to occur at a relatively small radio-frequency power for nuclei with large hyperfine coupling constants.

How the GTR behavior depends on the ^{14}N-quantum number (m_I) is discussed next. The ENDOR spectral changes by the ^{14}N-quantum number is described above. The spectra were influenced like the patterns summarized in Fig. 7, that is, the intensity height of each line is either increased or decreased, depending on the ^{14}N-

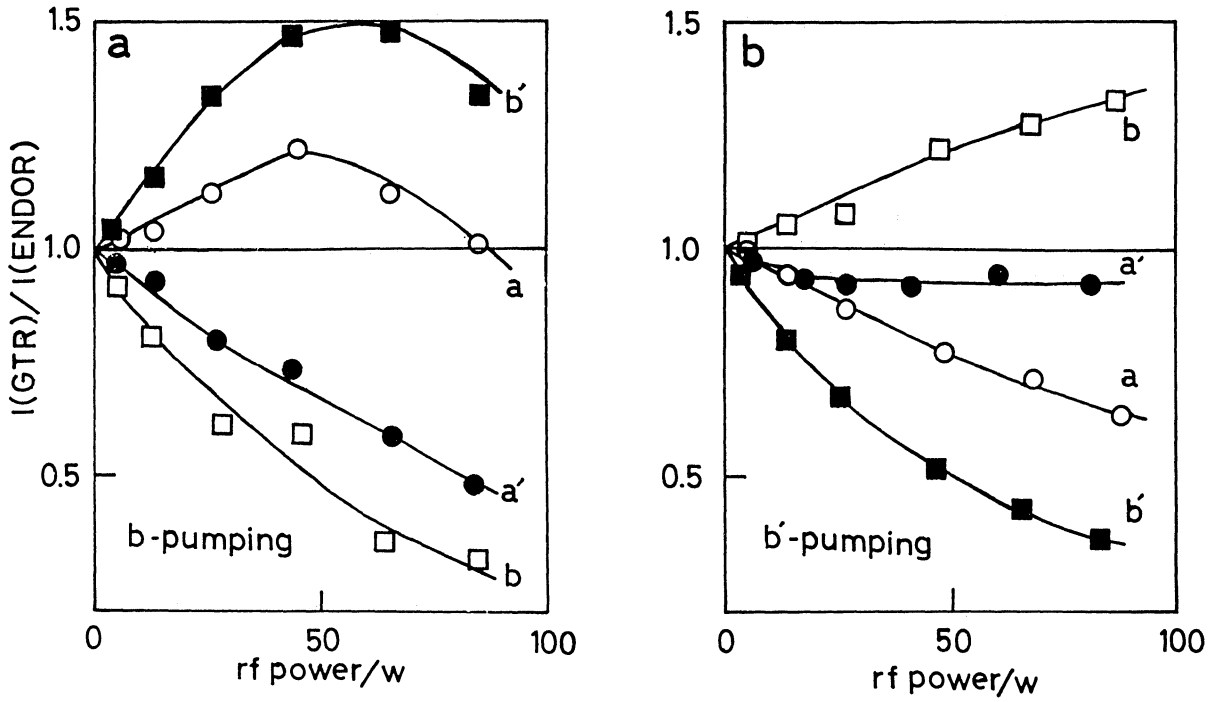

Fig. 8. Enhancement and de-enhancement of the GTR spectra with the inner paired ^{1}H-ENDOR lines (**b** and **b'**) pumped by the radio-frequency powers in the abscissa scale. ESR monitoring was set on the m_I=1 component. Compare with Fig. 4.

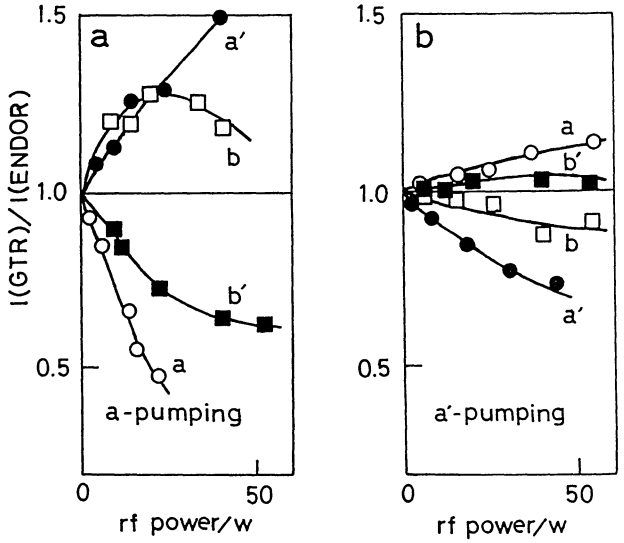

Fig. 9. Enhancement and de-enhancement of the GTR spectra with the outer paired ^{1}H-ENDOR lines (**a** and **a'**) pumped by the radio-frequency powers in the abscissa scale. ESR monitoring was set on the m_I=−1 component. Compare with Fig. 5.

quantum number (m_I) of the monitoring ESR and on the signs of the ^{1}H-hyperfine coupling constant (A_H). Regarding the GTR behavior, these cross relaxation effects should be combined, causing either more-enhanced or less-enhanced variations. This evidence is shown in Figs. 8 and 9. The experimental conditions for Fig. 8 were the same as those for Fig. 4, except for monitoring ESR. In the case of Fig. 8 the low-field ESR component (m_I=1) was monitored; line **b'** thus decreased, and line **b** increased due to the cross-relaxation effect (Fig. 7). Thus, the enhancement of the **b'** line or the de-enhancement of the b line is intensified by **b** pumping. This is the case of Fig. 8-a, which should be compared with Fig. 4-a. On the other hand, the opposite triple pumping (**b'** pumping) may give a dull behavior, like that shown in Fig. 8-b (compare with Fig. 4-b). Completely the same behaviors were also observed for high-field ESR monitoring (m_I=−1). As is hown in Fig. 9-a, enhancement of the **a'** line and the de-enhancement of the **a** line are intensified in the case of the **a** line pumping, because the line **a'** is already decreased and the line **a** increased by the cross relaxation (compare with Fig. 5-a). Fig 9-b should also be compared with Fig. 5-b. These findings belong to another type of three-spin effect in triple resonance spectroscopy.

In conclusion, by observing the ^{14}N- and ^{1}H-ENDOR spectra of DPNO, several interesting types of behavior were disclosed in ENDOR and GTR spectroscopies. The ^{14}N-hyperfine coupling constant detected by this ENDOR experiment is one of the smallest limits for the nitroxide radicals. The paired ^{14}N-ENDOR lines are distorted in intensity by cross relaxation in the ^{14}N nucleus and the unpaired electron. This effect is also present regarding the ^{1}H-ENDOR intensities. The double optimum temperatures for the ^{1}H-ENDOR lines were demonstrated, the higher one being due to the optimum energy relaxation of the ^{14}N nuclei and the

lower one due to that of the ^{1}H-spin system. These phenomena interelating two nuclei are interesting subjects concerning three-spin systems. In GTR experiments the intensity changes due to the radio-frequency-pumping power were analyzed in terms of the opposite signs of the hyperfine coupling constants, the enhancement saturation effect, and the effect of the cross relaxation. The latter two observations are pointed out here as a new interesting point concerning a three-spin system.

References

1) Y. Deguchi, *Bull. Chem. Soc. Jpn.*, **34**, 910 (1961).
2) Y. Deguchi, *Bull. Chem. Soc. Jpn.*, **35**, 260 (1962).
3) Y. Deguchi, *Bull. Chem. Soc. Jpn.*, **35**, 598 (1962).
4) J. Yamauchi, H. Nishiguchi, K. Mukai, Y. Deguchi, and H. Takaki, *Bull. Chem. Soc. Jpn.*, **40**, 2512 (1967).
5) J. Yamauchi, K. Okada, and Y. Deguchi, *Bull. Chem. Soc. Jpn.*, **60**, 483 (1987).
6) Y. Deguchi, K. Okada, J. Yamauchi, and K. Fujii, *Chem. Lett.*, **1983**, 1611.
7) H. Kurreck, B. Kirste, and W. Lubitz, "Electron Nuclear Double Resonance Spectroscopy of Radicals in Solutions," VCH Publisher, Inc., Weinheim (1988).
8) D. S. Leniart, J. C. Vedrine, and J. S. Hyde, *Chem. Phys. Lett.*, **6**, 637 (1970).
9) J. Yamauchi and Y. Deguchi, *Can. J. Chem.*, **66**, 1862 (1988).
10) The nitrogen hyperfine coupling constant is far larger than the proton ones. The ESR spectra, therefore, split into three groups which belong to m_I=1, 0, and −1 components.
11) F. Lendzian, M. Plato, and K. Mobius, *J. Magn. Reson.*, **44**, 20 (1981).
12) R. Biehl, K. Mobius, S. E. O'Connor, R. I. Walter, and H. Zimmermann, *J. Phys. Chem.*, **83**, 3449 (1979).
13) T. S. Lin, *J. Chem. Phys.*, **57**, 910 (1972).
14) E. G. Janzen and U. M. Oehler, *Chem. Lett.*, **1984**, 1233.
15) J. Yamauchi and Y. Deguchi, *Chem. Lett.*, **1985**, 111.
16) The former is the indirect ^{14}N and ^{1}H interaction through the hyperfine interactions ($A_N I_N S + A_H I_H S$) and the latter the direct ^{14}N and ^{1}H interaction of $J I_N I_H$ type.
17) K. Mobius and R. Biehl, "Multiple Electron Resonance Spectroscopy," ed by M. M. Dorio and J. H. Freed, Plenum Press, New York (1979), Chap. 14.